Magnetism in the Hubbard model: An effective spin Hamiltonian approach

Michael A. Tusch, Yolande H. Szczech, and David E. Logan
Physical and Theoretical Chemistry Laboratory, Oxford University, South Parks Road, Oxford OX1 3QZ, United Kingdom
(Received 9 August 1995; revised manuscript received 22 September 1995)

We present an approach to the magnetic properties of the half-filled Hubbard model, based on an approximate mapping of its low-energy transverse spin excitations on to those of an effective underlying Heisenberg model, but with effective spin interactions which are self-consistently determined and not confined solely to nearest-neighbor couplings. The mapping is exact in strong-coupling and is found to be accurate over a very wide range of interaction strengths, down to weak coupling. At zero temperature, it permits ready evaluation at finite U of the one-loop effects of zero-point spin fluctuations on, e.g., the sublattice magnetization. At finite temperatures, thermodynamic properties of the system in the thermal paramagnet are studied via a physically transparent Onsager reaction field approach, which amounts to a self-consistent treatment of paramagnetic spin correlations. This is central not only in recovering the correct dimensionality dependence of antiferromagnetic long-ranged order, but also for the $d=3$ case of primary interest here yields a Néel temperature in close agreement with known strong- and weak-coupling limits. Spin correlation functions and magnetic susceptibilities also show very good agreement with quantum Monte Carlo calculations over an appreciable temperature range in which the low-lying transverse spin excitations are thermally dominant.

I. INTRODUCTION

For several decades, the Hubbard model has provided a continuous and intense focus for understanding itinerant electron magnetism. It is specified by the Hamiltonian

$$H=-t\sum_{\langle ij\rangle,\sigma} c_{i\sigma}^{\dagger}c_{j\sigma}+U\sum_{i} n_{i\uparrow}n_{i\downarrow}, \tag{1.1}$$

with a nearest-neighbor (NN) hopping matrix element t, electron interactions embodied in the repulsive Hubbard U, and with the $\langle ij\rangle$ sum here over NN sites on a d-dimensional hypercubic lattice. Among the relatively few exact results known for $d>1$ is the familiar mapping,[1] at half-filling and in the strong-coupling interaction limit $U/t\rightarrow\infty$, on to the spin-$\frac{1}{2}$ antiferromagnetic (AF) Heisenberg model

$$H_{\mathrm{Heis}}=\frac{1}{2}\sum_{\substack{i,j\\(j\neq i)}} J_{ij}\mathbf{S}_i\cdot\mathbf{S}_j, \tag{1.2}$$

with $\mathbf{S}_i$ a spin-$\frac{1}{2}$ operator and purely NN exchange couplings given by $J_{ij}\equiv J_{\infty}=4t^2/U$. The quantum AF Heisenberg model is likewise far from understood, but much is known about its ground state and thermodynamic properties, both analytically and via Monte Carlo calculations (see, e.g., Ref. 2). Naturally, however, magnetic properties of the Hubbard model at finite U/t, where both charge and spin degrees of freedom are coupled by the interaction term in Eq. (1.1), are considerably less well understood.

In understanding finite-temperature properties of the Hubbard model, progress has been made over many years by functional integral techniques, usually based on a Hubbard-Stratonovich transformation or variants thereof, and generally formulated within the static approximation; see, e.g., Refs. 3–9 and references therein. A principal aim of such theories has been a determination of the Néel temperature for loss of AF long-ranged order (AFLRO), and thermodynamic properties of the paramagnetic phase in particular. However, while successful in some respects, they cannot provide a qualitatively correct description of the finite-U/t thermodynamics, since all yield the pure molecular field result for the NN Heisenberg model as $U/t\rightarrow\infty$, i.e., $T_N^{\mathrm{MF}}=Zt^2/U$, with $Z=2d$ the lattice coordination number. In $d=3$, this value is considerably in excess of the accepted $T_N\simeq 3.83t^2/U$ obtained from high-temperature series expansions,[10] and since the molecular field asymptote is insensitive to dimensionality, for $d\leqslant 2$ they fail to predict the absence of AFLRO required by the Mermin-Wagner theorem[11] for $T>0$.

We pursue here an entirely different approach to the half-filled Hubbard model, based on an approximate mapping of the low-energy transverse spin excitations at finite U/t on to those of an effective Heisenberg model, the U/t-dependent effective exchange couplings of which are self-consistently determined and not confined solely to NN interactions. To understand why such a procedure is likely to be viable, we refer first to recent work on the Hubbard model at $T=0$. As shown by several groups[12,13] for $d\geqslant 2$, a good description of the ground state of the model and its collective excitations is obtained by linearizing particle-hole excitations about a stable, broken symmetry unrestricted Hartree-Fock (UHF) ground state via a random phase approximation (RPA). For the strong-coupling limit in particular, it is found that the results of linear spin wave theory (LSW) for the pure AF Heisenberg model are thereby fully recovered, and it has been argued that UHF+RPA, together with zero-point spin fluctuations, is able to account for the physics of the half-filled Hubbard model at $T=0$.

LSW for the pure spin-$\frac{1}{2}$ AF Heisenberg model has itself proven highly successful,[2] as exemplified by the one-loop order effects of quantum zero-point fluctuations in reducing the sublattice magnetization m from its Néel value of unity. In $d=1$, where quantum fluctuations are at their most acute, the algebraically divergent spin wave amplitude as frequency $\omega\rightarrow 0$ naturally leads to a divergent reduction in m at

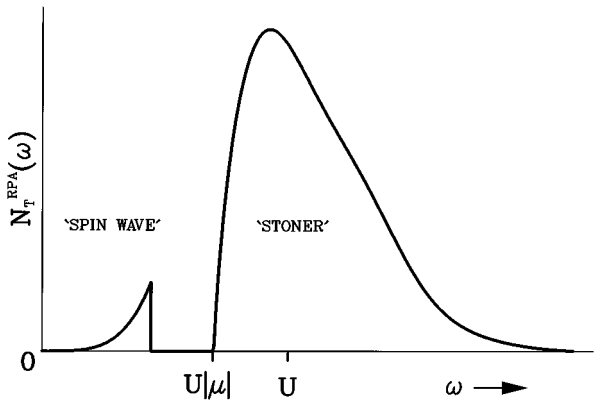

FIG. 1. Schematic illustration of the full RPA transverse spin spectrum for the half-filled Hubbard model. The single-particle band gap $\Delta = U|\mu|$, with $|\mu|$ the UHF local moment magnitude. (The relative intensity of the spin-wave-like band is greatly exaggerated: See text.)

$T=0$, reflecting the well-known absence of AFLRO in the exact solution. But for $d \geqslant 2$ the Néel state is robust, and the $T=0$ sublattice magnetization remains nonzero, commensurate with the widely held belief that the ground state of the spin-$\frac{1}{2}$ Heisenberg model has AFLRO;[2] for $d=2$, the one-loop sublattice magnetization is $m=0.607$, rising to $m=0.844$ for $d=3$ as spin fluctuation effects become less significant.[14] Most significantly, LSW results for the sublattice magnetization, spin wave velocity, and ground-state energy are in close agreement with quantum Monte Carlo (QMC) calculations for the pure AF Heisenberg model in $d=2$ (see, e.g., Ref. 2). Further, the logarithmic divergence of the spin wave amplitude for $d=2$ leads at any $T>0$ to a divergent magnetization reduction, consistent with the Mermin-Wagner theorem,[11] while for $d=3$, AFLRO is stable to thermal population of the spin waves up to the nonvanishing Néel temperature.

The fundamental collective excitations about the Néel state of the Heisenberg model are of course the N pure spin waves (with N the number of sites). For the finite-U/t Hubbard model, in contrast, there are N^2 collective particle-hole excitations, the nature and spectral density of which for both pure and site-disordered Hubbard models at half-filling in $d=3$ have recently been studied in detail at RPA level.[15] Figure 1 shows a schematic illustration of the resultant RPA excitation spectrum at moderate coupling U/t. This consists of two essential features. First, and our primary focus below, is a prominent low-energy spin-wave-like band, which extends to $\omega=0$ and is gapless. Second, and separated from the top of the spin-wave-like component, is a band of weakly renormalized Stoner-like excitations. The gap to these relatively high-energy excitations is on the order of the gap Δ in the single-particle UHF spectrum [which for half-filled bipartite lattices is nonzero for all $U>0$ (Ref. 16)], and their maximum spectral density typically occurs for $\omega \sim U$. Most importantly, it is found (see Sec. III) that the excitations comprising the low-ω band are, to a very good approximation, spin waves over a very wide range of interaction strengths U/t. This suggests that it should be possible to describe these excitations, which will govern the effect of zero-point fluctuations on the mean field ground state and dominate the low-temperature thermodynamics of the Hubbard model, in terms of an effective underlying Heisenberg model.

In Sec. II, we derive such an effective Hamiltonian, based on comparison of the site-resolved RPA equations for the Hubbard model with the LSW equations of an arbitrary Heisenberg model. The resultant $H_{\rm Heis}(U)$, which reduces in the strong-coupling limit $U/t \to \infty$ to the pure nearest-neighbor AF Heisenberg model, Eq. (1.2), is shown in Sec. III to reproduce quantitatively the lowest-N RPA excitations of the Hubbard model, down to weak-coupling interaction strengths $U/t \simeq 2-3$; and in Sec. III the U/t dependence of the effective exchange couplings is briefly discussed.

One advantage of an effective spin Hamiltonian is that it provides us with a potentially straightforward route to thermodynamic properties of the Hubbard model in a temperature regime dominated by the low-energy spin-wave-like excitations: We do not expect the accuracy of the effective exchange couplings to be sensitive to their extraction by comparison of linearized theories, so that thermodynamics of the model can be examined without explicit reference to, or the limitations of, the original RPA approximation.

This is considered in Sec. V, where an Onsager reaction field[17] (ORF) approach to the paramagnetic phase of the U/t-dependent $H_{\rm Heis}(U)$ is outlined briefly. This provides in effect a self-consistent modification of conventional molecular field theory to include the crucial effects of local spin correlations in the paramagnet. It is very simple, but physically transparent, and appears to transcend quite successfully the basic limitations of a crude molecular field approach, while remaining mean field in spirit. It is also rather rich. For example, $T_N(U)$ is reduced to zero for $d \leqslant 2$, consistent with the Mermin-Wagner theorem, while for $d=3$ the resultant Néel temperature as a function of U/t interpolates well between weak- and strong-coupling interaction strengths, yielding strong-coupling behavior very close to the best estimates of T_N obtained from high-temperature series expansions.[10]

The success of the approach is further demonstrated by comparison with quantum Monte Carlo calculations on the $d=3$ half-filled Hubbard model,[18,19] including the Néel $T_N(U)$ (Sec. V C), and the temperature dependence of intersite spin correlation functions and static susceptibilities (Sec. V D). The separation of energy scales alluded to above and discussed in Sec. II —between low-energy spin-wave-like excitations and higher-energy Stoner-like processes— translates thermally into the occurrence of an appreciable temperature interval over which thermodynamic properties of the paramagnetic phase of the Hubbard model are dominated by the spin degrees of freedom captured in the effective $H_{\rm Heis}(U)$, and are only weakly affected by the higher-energy excitations; in this temperature regime good agreement with QMC results is found. The results show clearly the importance of providing a sound description of local spin correlations in the paramagnet, for which we believe an ORF theory provides possibly the simplest, qualitatively correct treatment. A preliminary account of the work has been given in a recent paper.[21]

II. MAPPING TO AN EFFECTIVE HEISENBERG MODEL

We describe here a mapping of the low-energy transverse spin excitations of the half-filled Hubbard model for finite

U/t on to those of an effective Heisenberg model, Eq. (1.2), with no constraint to nearest-neighbor (NN) exchange couplings J_{ij}. This mapping is of course exact in the strong-coupling limit $U/t\rightarrow\infty$, and is found in practice to be accurate whenever there exists a discernible spin-wave-like band in the transverse excitation spectrum. As discussed in Sec. III, this is the case over a very wide U/t range extending down to weak interaction strengths for the pure Hubbard model. This feature is found also to persist for the ''dirty'' but magnetically ordered phases of site-disordered Hubbard models. Thus, although we focus here on the periodic system, we adopt a site-space representation appropriate more generally to disordered Hubbard models, in which context the mapping will be considered in a forthcoming paper.[20] We do, however, retain a two-sublattice basis appropriate to the nondisordered case, both to make contact with familiar LSW and for notational convenience.

We begin by treating the interaction term in Eq. (1.1) at the mean-field level of unrestricted HF, such that H may be rewritten as

$$H=H^0+\frac{1}{2}U\sum_{i,\sigma}\ \delta n_{i\sigma}\delta n_{i-\sigma}, \tag{2.1}$$

where

$$H^0=\sum_{i,\sigma}\ \epsilon_i n_{i\sigma}-t\sum_{\langle ij\rangle,\sigma}\ c^{\dagger}_{i\sigma}c_{j\sigma}+U\sum_{i}\ \left\{\frac{1}{2}\langle n_i\rangle n_i-2\langle\mathbf{S}_i\rangle\cdot\mathbf{S}_i\right\}. \tag{2.2}$$

In Eq. (2.2), $\langle\cdots\rangle$ denotes an expectation over the self-consistent UHF ground state, $\delta n_{i\sigma}=n_{i\sigma}-\langle n_{i\sigma}\rangle$, and c-number terms are omitted.

Solution of the mean-field UHF problem is straightforward for the half-filled pure Hubbard model on a bipartite lattice[16] —where any interaction strength $U/t>0$ leads to an Ising-like two-sublattice Néel AF— but is in general rather more complex. In particular, a rich phase diagram at zero temperature for the Gaussian site-disordered Hubbard model has been obtained,[22] where the dominant magnetic phase in the disorder-interaction plane is a dirty AF. As shown in Ref. 22, however, the UHF ground states for this model are also Ising-like at half-filling (a property we expect to be generic to purely site-disordered Hubbard models), with local magnetic moments lying along a common z axis and $\langle S^{\rm tot}_z\rangle=\Sigma_i\langle S_{iz}\rangle=0$. This is the only property of the mean-field ground state of which we shall make use here, so that this additional class of disordered Hubbard models can be encompassed by assuming a UHF magnetic ground state characterized by a set of self-consistently determined local moments $\{\mu_i\}$ with $\mu_i\equiv 2\langle S_{iz}\rangle$. For Ising-like ground states, the UHF single-particle wave functions are pure spin orbitals, given via $|\Psi_{\alpha\sigma}\rangle=\Sigma_i f_{i\alpha\sigma}|\phi_{i\sigma}\rangle$ in a site basis, with associated eigenvalues $\{\epsilon_{\alpha\sigma}\}$ and pure real eigenvector coefficients $\{f_{i\alpha\sigma}\}$. The mean-field local moments are obtained from the UHF self-consistency condition

$$\mu_i=\sum_{\alpha\sigma<F}\ \sigma|f_{i\alpha\sigma}|^2, \tag{2.3}$$

with F the Fermi level.

Collective excitations about the UHF ground state are obtained within the RPA by linearizing the equations of motion for particle-hole pairs created and destroyed in the UHF vacuum. With UHF state creation and destruction operators defined via

$$c^{\dagger}_{\alpha\sigma}=\sum_i\ f_{i\alpha\sigma}c^{\dagger}_{i\sigma};\quad c_{\alpha\sigma}=\sum_i\ f_{i\alpha\sigma}c_{i\sigma}, \tag{2.4}$$

a canonical transformation to particles and holes is made:

$$c_{\alpha\sigma}=\theta(\alpha-F)a_{\alpha\sigma}+\theta(F-\alpha)b^{\dagger}_{\alpha\sigma}, \tag{2.5a}$$

$$c^{\dagger}_{\alpha\sigma}=\theta(\alpha-F)a^{\dagger}_{\alpha\sigma}+\theta(F-\alpha)b_{\alpha\sigma}. \tag{2.5b}$$

Linearization of the equations of motion given via the commutators $[H,O]$, where the particle-hole (p-h) pair creation or destruction operator $O\in\{a^{\dagger}_{\alpha\sigma}b^{\dagger}_{\beta\sigma'},b_{\beta\sigma'}a_{\alpha\sigma}\}$, leads straightforwardly to the generalized RPA equations; see, e.g., Ref. 23. Alternatively, and equivalently, an effective quadratic boson Hamiltonian may be introduced (see, e.g., Ref. 24) for which the equations of motion for the operators O, within the quasiboson approximation, are precisely the RPA equations. This Hamiltonian is readily shown to be given by

$$H_{\rm RPA}=\frac{1}{2}\boldsymbol{\zeta}^{\dagger}\boldsymbol{\Pi}^{-1}(0)\boldsymbol{\zeta}, \tag{2.6}$$

where the $2N^2$-dimensional vector $\boldsymbol{\zeta}=(a^{\dagger}_{\alpha}b^{\dagger}_{\beta},\ldots,b_{\beta}a_{\alpha},\ldots)$ with $\alpha>F>\beta$; the σ-index is temporarily suppressed for notational convenience. $\boldsymbol{\Pi}(\omega)$ is the particle-hole component of the time-ordered polarization propagator within the RPA approximation, and is given by

$$\begin{aligned}\Pi_{\alpha\beta;\lambda\mu}(\omega)&=i\int dt e^{i\omega t}\langle 0|\mathscr{T}c^{\dagger}_{\beta}(t)c_{\alpha}(t)c^{\dagger}_{\lambda}c_{\mu}|0\rangle\\&=\sum_{n>0}\left\{\frac{\langle 0|c^{\dagger}_{\beta}c_{\alpha}|n\rangle\langle n|c^{\dagger}_{\lambda}c_{\mu}|0\rangle}{(E_n-E_0)-\omega-i\eta}\right.\\&\quad\left.+\frac{\langle 0|c^{\dagger}_{\lambda}c_{\mu}|n\rangle\langle n|c^{\dagger}_{\beta}c_{\alpha}|0\rangle}{(E_n-E_0)+\omega-i\eta}\right\},\end{aligned} \tag{2.7}$$

where $|0\rangle$ and $|n\rangle$ are, respectively, the RPA ground and excited states, and with Greek subscripts denoting UHF states in the particle-hole subspace $\alpha\lambda>F>\beta\mu$ and $\alpha\lambda<F<\beta\mu$. $\boldsymbol{\Pi}(\omega)$ is obtained most conveniently in terms of the corresponding UHF propagator

$$\begin{aligned}{}^0\Pi_{\alpha\beta;\lambda\mu}(\omega)&=\delta_{\alpha\lambda}\delta_{\beta\mu}\left\{\frac{\theta(\alpha-F)\,\theta(F-\beta)}{(\epsilon_{\alpha}-\epsilon_{\beta})-\omega-i\eta}\right.\\&\quad\left.+\frac{\theta(\beta-F)\,\theta(F-\alpha)}{(\epsilon_{\beta}-\epsilon_{\alpha})+\omega-i\eta}\right\}\end{aligned} \tag{2.8}$$

by solving a Bethe-Salpeter equation with interaction kernel

$$V_{\alpha\beta;\lambda\mu}(\omega)=-\langle\alpha\mu|V|\lambda\beta\rangle+\langle\mu\alpha|V|\lambda\beta\rangle, \tag{2.9}$$

where $V=H-H_0$, i.e., $\langle\alpha\mu|V|\lambda\beta\rangle=U\Sigma_i f_{i\alpha}f_{i\beta}f_{i\lambda}f_{i\mu}$. This leads[23] to the simple expression $\boldsymbol{\Pi}^{-1}(\omega)={}^0\boldsymbol{\Pi}^{-1}(\omega)-\mathbf{V}$. Taking matrix elements of the set of commutators $[H_{\rm RPA},\boldsymbol{\zeta}]$ between RPA ground and excited states, and enforcing the quasiboson commutation relation

$$[a_\alpha^\dagger b_\beta^\dagger, b_\gamma a_\delta] \simeq \langle [a_\alpha^\dagger b_\beta^\dagger, b_\gamma a_\delta] \rangle = \delta_{\alpha\delta}\delta_{\beta\gamma} \quad (2.10)$$

then leads directly to the RPA equations. As implied by Eq. (2.7), the eigenvalues of H_{RPA} thus correspond to the poles of $\mathbf{\Pi}(\omega)$, i.e., the RPA collective particle-hole excitation energies.

For an Ising-like UHF ground state, the susceptibility matrix $\mathbf{\Pi}(\omega)$ —with linear dimension $2N^2$— block diagonalizes into a transverse spin sector and a mixed charge-longitudinal spin sector ($\mathbf{\Pi}^{LC}$), each of dimension N^2. The transverse susceptibility matrix further decouples into two $N^2/2$-dimensional blocks denoted by $\mathbf{\Pi}^{-+}(\omega)$ and $\mathbf{\Pi}^{+-}(\omega)$, where

$$\Pi^{-+}_{\alpha\beta;\lambda\mu}(\omega) = i \int dt e^{i\omega t} \langle 0 | \mathscr{T} c^\dagger_{\beta\downarrow}(t) c_{\alpha\uparrow}(t) c^\dagger_{\lambda\uparrow} c_{\mu\downarrow} | 0 \rangle, \quad (2.11a)$$

with the spin indices now restored, and

$$\Pi^{-+}_{\alpha\beta;\lambda\mu}(\omega) = \Pi^{+-}_{\mu\lambda;\beta\alpha}(-\omega). \quad (2.11b)$$

The transverse sectors $\mathbf{\Pi}^{-+}(\omega)$ and $\mathbf{\Pi}^{+-}(\omega)$ contain low-energy excitations extending down to zero frequency, as implied by the existence of Goldstone modes in the transverse spin spectrum. In contrast, $\mathbf{\Pi}^{LC}(\omega)$ consists of weakly renormalized HF excitations across the band gap $\Delta = U|\mu|$ in the single-particle UHF spectrum, with a corresponding spectral density which is thus nonzero only for $\omega \gtrsim \Delta$. The decoupling of the $\mathbf{\Pi}$ matrix implies that H_{RPA} is itself separable, viz.,

$$H_{\mathrm{RPA}} = H^{-+}_{\mathrm{RPA}} + H^{+-}_{\mathrm{RPA}} + H^{LC}_{\mathrm{RPA}}, \quad (2.12)$$

where each component has the form of Eq. (2.6), with $\mathbf{\Pi}^{-1}(0)$ appropriate to the particular sector. The lowest-energy excitations clearly occur in the transverse sectors H^{-+}_{RPA} and H^{+-}_{RPA}. These spin-flip excitations are expected to be dominant for all but the lowest interaction strengths and up to temperatures on the order of the single-particle gap; we therefore focus on them below.

As a prerequisite to establishing a connection to linear spin wave theory, our aim now is to transform H_{RPA} from the UHF state basis to a site basis. To this end we first extend formally the Hilbert space to include particle-particle (p-p) and hole-hole (h-h) excitations. These are not of course included within RPA, and in the UHF state representation fully decouple from particle-hole excitations [since the interaction kernel, Eq. (2.9), couples only p-h excitations]. In Eq. (2.6), therefore, $\boldsymbol{\zeta}$ is formally extended to include terms of form $a^\dagger_\alpha a_\lambda$ ($\alpha\lambda > F$) and $b_\beta b^\dagger_\mu$ ($\beta\mu < F$), while these excitations are simultaneously suppressed by associating with them an arbitrarily large energy. The extended RPA Hamiltonian matrix is block diagonal, with linear dimension $4N^2$, consisting of a $2N^2$-dimensional p-h component, and a $2N^2$-dimensional, diagonal block with infinite diagonal elements corresponding to p-p and h-h excitations. We also extend the quasiboson approximation [Eq. (2.10)] to describe the additional processes by requiring that all p-p and h-h operators commute with p-h operators

$$[a^\dagger_\alpha a_\lambda, a^\dagger_\gamma b^\dagger_\beta] \simeq \langle [a^\dagger_\alpha a_\lambda, a^\dagger_\gamma b^\dagger_\beta] \rangle = 0, \text{ etc.} \quad (\alpha\lambda\gamma > F > \beta), \quad (2.13)$$

whence the resultant states thus decouple into disjoint p-h and p-p/h-h sets. Since extension of the Hilbert space is purely a formal device, the equations of motion for the p-h operators $O \in \{a^\dagger_{\alpha\sigma} b^\dagger_{\beta\sigma'}, b_{\beta\sigma'} a_{\alpha\sigma}\}$, obtained from the enlarged H_{RPA} using the quasiboson approximation, again lead directly to the RPA equations.

We now consider the site resolution of $\mathbf{\Pi}^{-+}(\omega)$, and hence H^{-+}_{RPA}. A matrix $\mathbf{P}(\omega)$, with elements $P_{ij;kl}(\omega)$ and linear dimension $2(N^2/2)$, is defined via the orthogonal transformation

$$\mathbf{P}(\omega) = \mathbf{T}^T \mathbf{\Pi}^{-+}(\omega) \mathbf{T}, \quad (2.14)$$

where

$$T_{\alpha\beta;ij} = T^T_{ij;\alpha\beta} = f_{i\alpha\uparrow} f_{j\beta\downarrow} \quad (2.15)$$

and $\mathbf{\Pi}^{-+}(\omega)$ is given by Eq. (2.11a), with *no* restrictions on the UHF state indices. From Eqs. (2.15) and (2.11a), the matrix elements of $\mathbf{P}(\omega)$ may be written in the form

$$P_{ij;kl}(\omega) = \sum_n \left\{ \frac{\langle 0 | c^\dagger_{j\downarrow} c_{i\uparrow} | n \rangle \langle n | c^\dagger_{k\uparrow} c_{l\downarrow} | 0 \rangle}{(E_n - E_0) - \omega - i\eta} + \frac{\langle 0 | c^\dagger_{k\uparrow} c_{l\downarrow} | n \rangle \langle n | c^\dagger_{j\downarrow} c_{i\uparrow} | 0 \rangle}{(E_n - E_0) + \omega - i\eta} \right\}, \quad (2.16)$$

where the N^2 states $\{|n\rangle\}$ span the enlarged Hilbert space of two-fermion excitations and fully decouple into p-h and p-p/h-h sets. However, since states belonging to the latter set are associated with arbitrarily large eigenvalues $(E_n - E_0)$, the elements $P_{ij;kl}(\omega)$ receive nonvanishing contributions *only* from the particle-hole sector. $\mathbf{P}(\omega)$ is thus precisely the site-resolved particle-hole RPA susceptibility: The formal extension of the Hilbert space naturally has no effect on the RPA collective excitation spectrum.

Application of the above transformation to H^{-+}_{RPA} yields

$$H^{-+}_{\mathrm{RPA}} = \frac{1}{2} (\boldsymbol{\zeta}^\dagger \mathbf{T}) \mathbf{P}^{-1}(0) (\mathbf{T}^T \boldsymbol{\zeta}). \quad (2.17)$$

Extraction of the particle-hole sector of H^{-+}_{RPA} in a site representation is in general complex, but ready progress may be made by introducing the central approximation of the present theory, whose accuracy can be verified explicitly as detailed in Sec. III. This is to posit for finite U/t that the N lowest-frequency transverse spin excitations are largely spin-wave-like, which implies [see (2.16)] that the associated N lowest-energy states $|n\rangle$ are connected to the ground state $|0\rangle$ by excitations with weight almost exclusively in the *on*-site spin-flip subspace; i.e., for $j \neq i$,

$$\langle 0 | c^\dagger_{i\uparrow} c_{i\downarrow} | n \rangle \gg \langle 0 | c^\dagger_{i\uparrow} c_{j\downarrow} | n \rangle \simeq 0;$$

and, conversely, that the remaining $N^2/2 - N$ excitations in the p-h sector have virtually no weight in the on-site spin-flip subspace; i.e., for at least some $j \neq i$,

$$\langle 0 | c^\dagger_{i\uparrow} c_{j\downarrow} | n' \rangle \gg \langle 0 | c^\dagger_{i\uparrow} c_{i\downarrow} | n' \rangle \simeq 0.$$

If the above conditions are satisfied, then from the Lehmann representation [Eq. (2.16)] for $\mathbf{P}(\omega)$ it is clear that elements such as $P_{ii;jk}(\omega) \simeq 0$ for $j \neq k$; i.e., $\mathbf{P}(\omega)$ is ap-

proximately block diagonal, with an $N\times N$ block containing elements $P_{ii;jj}(\omega)\equiv\chi_{ij}(\omega)$ which are thus dominated by the low-energy spin-wave-like excitations. In contrast, the second block in $\mathbf{P}(\omega)$ is dominated by the remaining $N^2/2-N$ transverse p-h excitations which, akin to those of $\mathbf{\Pi}^{LC}(\omega)$, are high-energy Stoner-like excitations with nonvanishing spectral weight only for $\omega\gtrsim\Delta=U|\mu|$. The approximation described is clearly exact in strong-coupling $U/t\rightarrow\infty$, where $P_{ij;kl}(\omega)=\delta_{ij}\delta_{kl}P_{ii;kk}(\omega)$ and only the low-energy sector survives. The $N^2\times N^2$ matrix $\mathbf{P}(0)$ then has N nonzero eigenvalues associated with N spin wave excitations, and N^2-N zero eigenvalues, of which $N^2/2$ are trivially associated with the suppressed p-p/h-h excitations, while the remaining $N^2/2-N$ zero eigenvalues likewise reflect the infinite energy associated with the Stoner-like processes as $U/t\rightarrow\infty$.

Focusing therefore on the low-energy spin-wave-like contributions to H^{-+}_{RPA} [Eq. (2.17)] and H^{+-}_{RPA}, by retaining only the on-site components $P_{ii;jj}\equiv\chi_{ij}$ in $\mathbf{P}(0)$, leads directly to an approximate spin wave Hamiltonian

$$H_{\mathrm{SW}}=\frac{1}{2}\sum_{i,j}\ [\boldsymbol{\chi}^{-1}(0)]_{ij}\{S_i^+S_j^-+S_i^-S_j^+\},\qquad(2.18)$$

where the second term follows from analogous consideration of $\mathbf{\Pi}^{+-}(\omega)$ and hence H^{+-}_{RPA}. Note that the operators in Eq. (2.18) are not full spin-$\frac{1}{2}$ operators; rather, they obey the quasiboson commutation relation

$$[S_i^+,S_j^-]=\mu_i\delta_{ij}=\langle[S_i^+,S_j^-]\rangle,\qquad(2.19)$$

as may be verified explicitly by transformation of Eq. (2.19) back to a UHF state basis and application of Eqs. (2.10) and (2.13).

Proceeding analogously to LSW, we now divide the system into two sublattices A and B, such that the mean-field $\langle S_{iz}\rangle=\tau_i|\mu_i|/2$ with $\tau_i=+(-)$ for sites belonging to sublattice A (B), and with spin raising-lowering operators given by

$$S_i^+=\sqrt{|\mu_i|}\begin{cases}d_i & :i\in A,\\ d_i^\dagger & :i\in B,\end{cases}\qquad S_i^-=\sqrt{|\mu_i|}\begin{cases}d_i^\dagger & :i\in A,\\ d_i & :i\in B,\end{cases}\qquad(2.20)$$

in terms of the Bose operators $d_i/d_i^\dagger$ (such that the Bose commutation $[d_i,d_j^\dagger]=\delta_{ij}$ yields correctly Eq. (2.19)). Equation (2.18) for H_{SW} then becomes

$$H_{\mathrm{SW}}=\frac{1}{2}\sum_{\substack{i,j\\ \tau_i=\tau_j}}C_{ij}(d_i^\dagger d_j+d_id_j^\dagger)+\frac{1}{2}\sum_{\substack{i,j\\ \tau_i\neq\tau_j}}C_{ij}(d_id_j+d_i^\dagger d_j^\dagger),\qquad(2.21a)$$

with

$$C_{ij}=\sqrt{|\mu_i\mu_j|}[\boldsymbol{\chi}^{-1}(0)]_{ij}.\qquad(2.21b)$$

We now show that H_{SW} is precisely the LSW Hamiltonian corresponding to the effective Heisenberg model

$$H_{\mathrm{Heis}}(U)=\sum_{\substack{i,j\\ (j\neq i)}}\ [\ \chi^{-1}(0)]_{ij}\tilde{\mathbf{S}}_i\cdot\tilde{\mathbf{S}}_j,\qquad(2.22)$$

where $\tilde{\mathbf{S}}_i=|\mu_i|\mathbf{S}_i$ and $\mathbf{S}_i$ is a spin-$\frac{1}{2}$ operator, such that $\langle\tilde{S}_{iz}\rangle=(\tau_i/2)|\mu_i|$ yields correctly the UHF mean field local moment for any site. The linear Holstein-Primakoff transformation for H_{Heis} corresponds to $\tilde{S}_{iz}=\frac{1}{2}\mu_i-\tau_id_i^\dagger d_i$ and $\tilde{S}_i^\pm$ given by Eq. (2.20) in terms of the Bose operators $d_i/d_i^\dagger$. Applied to Eq. (2.22) (and dropping c-number terms) this yields precisely Eq. (2.21a) with

$$C_{ij}=-\tau_i\delta_{ij}\left\{\sum_{\substack{k\\ (\neq i)}}[\boldsymbol{\chi}^{-1}(0)]_{ik}\tau_k|\mu_k|\right\}+(1-\delta_{ij})\sqrt{|\mu_i\mu_j|}[\boldsymbol{\chi}^{-1}(0)]_{ij}\qquad(2.23a)$$

$$=\sqrt{|\mu_i\mu_j|}[\boldsymbol{\chi}^{-1}(0)]_{ij}.\qquad(2.23b)$$

Equation (2.23b) reflects the existence of two (zero-frequency) Goldstone modes in the spectrum of H_{SW}, corresponding to global rotations of the UHF mean field spins, as required by the Ising-like nature of the UHF state for all $U/t>0$; this is embodied formally in

$$\sum_k\ [\boldsymbol{\chi}^{-1}(0)]_{ik}\mu_k=0\qquad(2.24)$$

(for all i), from which follows directly the equality of Eqs. (2.23a) and (2.23b).

Finally, we rewrite Eq. (2.22) in terms of the spin-$\frac{1}{2}$ operators as

$$H_{\mathrm{Heis}}(U)=\frac{1}{2}\sum_{\substack{i,j\\ (j\neq i)}}J_{ij}(U)\mathbf{S}_i\cdot\mathbf{S}_j,\qquad(2.25a)$$

with exchange couplings given by

$$J_{ij}=2|\mu_i\mu_j|[\boldsymbol{\chi}^{-1}(0)]_{ij}\quad:j\neq i.\qquad(2.25b)$$

This is the effective Heisenberg model we seek. Further, the Bethe-Salpeter equation for the RPA $\boldsymbol{\chi}(\omega)$ in a site representation is given by the familiar form

$$\boldsymbol{\chi}^{-1}(\omega)={}^0\boldsymbol{\chi}^{-1}(\omega)-U\mathbf{1},\qquad(2.26)$$

(where $[\mathbf{1}]_{ij}=\delta_{ij}$) in terms of its UHF counterpart ${}^0\boldsymbol{\chi}$ (see, e.g., Ref. 25), from which it follows that, for $j\neq i$, $[\ \chi^{-1}(0)]_{ij}\equiv[{}^0\boldsymbol{\chi}^{-1}(0)]_{ij}$. Knowledge of the UHF susceptibility matrix ${}^0\boldsymbol{\chi}(\omega)\equiv{}^0\boldsymbol{\chi}^{-+}(\omega)$ with elements given by

$${}^0\chi_{ij}^{-+}(\omega)=\sum_{\alpha>F>\beta}\left\{\frac{f_{i\alpha\uparrow}f_{j\alpha\uparrow}f_{i\beta\downarrow}f_{j\beta\downarrow}}{(\epsilon_{\alpha\uparrow}-\epsilon_{\beta\downarrow})-\omega-i\eta}+\frac{f_{i\alpha\downarrow}f_{j\alpha\downarrow}f_{i\beta\uparrow}f_{j\beta\uparrow}}{(\epsilon_{\alpha\downarrow}-\epsilon_{\beta\uparrow})+\omega-i\eta}\right\}\qquad(2.27)$$

in terms of the UHF eigenvalues and eigenvector coefficients, together with the mean field local moments $\{|\mu_i|\}$, thus enables a direct determination of the effective exchange couplings $\{J_{ij}\}$.

Before proceeding with a quantitative investigation of the accuracy of the above mapping at finite U/t, it is worth noting that the relation between the effective exchange couplings and the inverse of the static RPA susceptibility, Eq. (2.25b), is exact for the spin-$\frac{1}{2}$ Heisenberg model, to which

the Hubbard model reduces exactly in strong coupling. The RPA $\boldsymbol{\chi}^{-1}(0)$ appropriate to this model is readily shown to have matrix elements

$$[\boldsymbol{\chi}^{-1}(0)]_{ij} = -\frac{1}{2}\delta_{ij}\tau_i\sum_j J_{ij}\tau_j + \frac{1}{2}J_{ij}. \tag{2.28}$$

Use of Eq. (2.28) in Eq. (2.21) (with $|\mu_i|=1\forall i$ as appropriate for $U/t\to\infty$), followed by Fourier transformation and diagonalization, then leads directly to the familiar LSW dispersion given, for NN $J_{ij}\equiv J_\infty$, by

$$\omega_{\mathbf{q}} = \pm dJ_\infty\sqrt{1-\gamma_{\mathbf{q}}^2}, \tag{2.29}$$

where $\gamma_{\mathbf{q}}=d^{-1}\Sigma_{\alpha=1}^{d}\cos(q_\alpha a)$ with d the lattice dimensionality and a the lattice constant.

III. ACCURACY OF THE MAPPING

We have thus constructed an approximate mapping of the low-energy transverse spin excitations of the half-filled Hubbard model for finite U/t, on to those of an effective Heisenberg model whose exchange couplings [Eq. (2.25b)] are derived from the static RPA spin susceptibility of the original model (and are not therefore confined solely to nearest-neighbor interactions). Before discussing the resultant $J_{ij}(U)$'s, however, we first ascertain the accuracy of the mapping, and its range of validity in U/t.

The basic idea for any given $U/t>0$ is thus to compare directly the full RPA transverse spin spectrum of the Hubbard model with the linear spin wave spectrum of the effective $H_{\mathrm{Heis}}(U)$, Eq. (2.25). The former is denoted by $N_T^{\mathrm{RPA}}(\omega)$, the latter by $N_T^{\mathrm{LSW}}(\omega)$, with $N_T(\omega)=N_T(-\omega)$ in each case. $N_T^{\mathrm{LSW}}(\omega)=\Sigma_{\mathbf{q}}\delta(\omega-\omega_{\mathbf{q}})$ is obtained directly from the eigenvalues $\{\omega_{\mathbf{q}}\}$ of H_{SW}, Eq. (2.21), by a conventional Bogoliubov transformation; in the strong-coupling limit $U/t\to\infty$, $\omega_{\mathbf{q}}$ reduces to Eq. (2.29) with $J_\infty=4t^2/U$. The full RPA transverse spin spectrum $N_T^{\mathrm{RPA}}(\omega)=\Sigma_n\delta(\omega-\omega_n)$ is obtained most efficiently from the ω poles $\{\omega_n\}$ of the transverse susceptibility matrices $\boldsymbol{\chi}^{-+}(\omega)$ [Eqs. (2.26), (2.27)] and $\boldsymbol{\chi}^{+-}(\omega)$. Since $\boldsymbol{\chi}^{-+}(\omega)=\boldsymbol{\chi}^{+-}(-\omega)$ [see Eq. (2.11b)], the full $N_T^{\mathrm{RPA}}(\omega)$ may be derived from the poles of $\boldsymbol{\chi}(\omega)\equiv\boldsymbol{\chi}^{-+}(\omega)$ alone. The latter are readily obtained by noting that, because the same unitary transformation diagonalizes both $\boldsymbol{\chi}$ and ${}^0\boldsymbol{\chi}$, the matrix elements of the RPA susceptibility may be written in terms of the eigenvalues $\{\lambda_\gamma\}$ and associated eigenvectors $\{\mathbf{V}_\gamma\}$ of ${}^0\boldsymbol{\chi}$:

$$\chi_{ij}(\omega)=\sum_\gamma V_{i\gamma}(\omega)\frac{\lambda_\gamma(\omega)}{1-U\lambda_\gamma(\omega)}V_{j\gamma}(\omega). \tag{3.1}$$

The poles $\{\omega_n\}$ of $\boldsymbol{\chi}(\omega)$ are therefore given by

$$1-U\lambda_\gamma(\omega_n)=0. \tag{3.2}$$

Thus, $N_T^{\mathrm{RPA}}(\omega)$ may be obtained by examining the ω dependence of the eigenvalues of the UHF ${}^0\boldsymbol{\chi}(\omega)$.[15] Further, analysis of the behavior of any $\lambda_\gamma(\omega_n)$ near $\lambda(\omega)=1/U$ shows[15] that the on-site spin-flip or spin wave character of the corresponding RPA excitation is given by

$$\Omega(\omega_n)=\left[U^2\left|\frac{\partial\lambda}{\partial\omega}\right|_{\omega_n}\right]^{-1}$$
$$=\theta(\omega_n)\sum_i|\langle 0|S_i^-|n\rangle|^2$$
$$+\theta(-\omega_n)\sum_i|\langle 0|S_i^+|n\rangle|^2 \tag{3.3}$$

[with $|n\rangle$ the RPA excited state corresponding to the pole at $\omega_n=E_n-E_0$ in $\boldsymbol{\chi}(\omega)$; see Eq. (2.16) for $\chi_{ij}(\omega)\equiv P_{ii;jj}(\omega)$]. $\Omega(\omega_n)$ measures the weight of the RPA excitation in the subspace of on-site spin flips, such that excitations which are pure spin waves have $\Omega=1$,[15] while excitations with $\Omega\ll 1$ have significant off-site "charge-transfer" character.

Figure 1 gives a schematic illustration of the full $N_T^{\mathrm{RPA}}(\omega)$ which results. This consists of two essential components. First, a spin-wave-like band at low ω, containing precisely N excitations and extending down to $\omega=0$, as implied by the presence for all $U/t>0$ of a Goldstone mode (see Sec. II). Second, a band consisting of $(N/2)(N-2)$ Stoner-like excitations —stemming largely from intersite or charge-transfer spin-flip excitations, i.e., weakly renormalized UHF transverse excitations across the single-particle band gap. For the pure Hubbard model, the band gap $\Delta=U|\mu|$ is given by the UHF local moment self-consistency relation[12]

$$1=\frac{U}{N}\sum_{\mathbf{q}\in\,\mathrm{MBZ}}[\tfrac{1}{4}\Delta^2+\epsilon_{\mathbf{q}}^2]^{-1/2}, \tag{3.4}$$

where $\epsilon_{\mathbf{q}}=-2dt\gamma_{\mathbf{q}}$ are the tight-binding energies of the unperturbed ($U=0$) bipartite lattice. Δ is nonzero for all $U>0$,[12] whence the Stoner-like band begins at $\omega\sim\Delta$ as indicated in Fig. 1, and has maximum spectral weight typically around $\omega\sim U$. In the strong-coupling limit the single-particle gap $\Delta(U)\to\infty$, eliminating the Stoner-like band, leaving solely the N-excitation spin wave component given by Eq. (2.29), as discussed above. At finite U/t the Stoner-like band mixes with the pure spin wave band but of central importance is the existence, over a very wide range of interaction strengths, of a true gap separating the two bands, as illustrated in Fig. 1. Numerical studies using 2^{15} $\mathbf{q}$ points indicate that the spectral gap in $N_T^{\mathrm{RPA}}(\omega)$ persists down to very-weak-coupling strengths of around $U/t\simeq 2$, i.e., U around one-sixth of the unperturbed $d=3$ band width $B=12t$.

The occurrence of a spectral gap shows the persistent separation of energy scales for the spin-wave-like and Stoner-like excitations, extending down to weak-coupling interaction strengths. To examine the accuracy with which the former are reproduced by the effective Heisenberg model, Fig. 2 shows the low-ω portion of the transverse excitation spectrum $N_T^{\mathrm{RPA}}(\omega)$, containing the first N excitations, obtained directly via a pole search on Eq. (2.26) using 2^{15} $\mathbf{q}$ points and for interaction strengths $U/t=20,12$, and 6 (the spectra are normalized and have been smoothed conventionally using Lorentzians with half-widths on the order of the local level spacing). These are to be compared with $N_T^{\mathrm{LSW}}(\omega)$ for the corresponding effective Heisenberg model

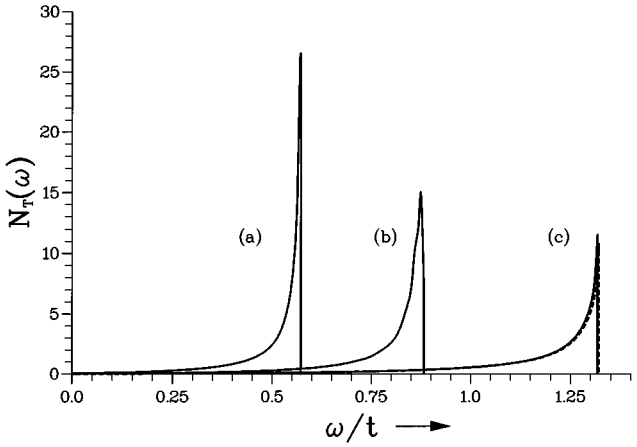

FIG. 2. $N_T^{\mathrm{RPA}}(\omega)$ (solid lines) and $N_T^{\mathrm{LSW}}(\omega)$ (dashed lines) vs ω/t for the half-filled Hubbard model, with $U/t=20$ (a), 12 (b), and 6 (c).

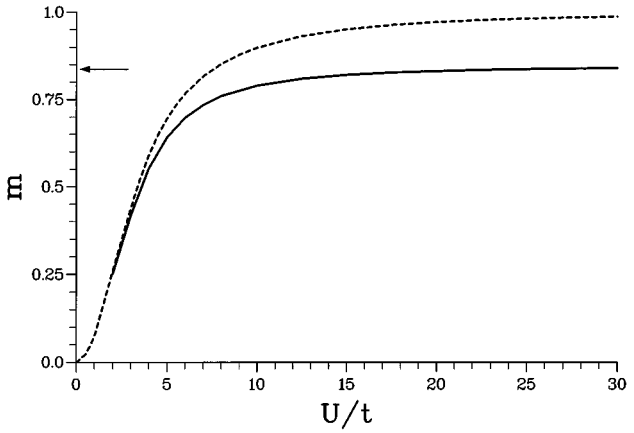

FIG. 3. Sublattice magnetization m vs U/t , obtained via one-loop inclusion of zero-point transverse spin fluctuations. Also shown is the UHF limit, $m\equiv|\mu|$ (dashed line). The strong-coupling limit $m=0.844$ is indicated by an arrow.

$H_{\mathrm{Heis}}(U)$. In Fig. 2 explicit comparison of $N_T^{\mathrm{RPA}}(\omega)$ and $N_T^{\mathrm{LSW}}(\omega)$ is in fact shown only for $U/t=6$, since for stronger interactions the spectra are indistinguishable; for $U/t=6$ itself the difference is barely discernible. Even for weak coupling, e.g., $U/t=3$, the agreement is good, with the spectral features of $N_T^{\mathrm{RPA}}(\omega)$ well reproduced by $N_T^{\mathrm{LSW}}(\omega)$, save for a slight net shift to lower energy, reflecting level repulsion with the approaching upper Stoner-like band and similar quality of comparison occurs for $U/t=2$.

The degree to which the *character* of the lowest-N RPA excitations is reproduced by $N_T^{\mathrm{LSW}}(\omega)$ may also be assessed by examining $\Omega(\omega)$, Eq. (3.3), as discussed above: A value of $\Omega(\omega)\simeq 1$ for ω in the lower band indicates the clear dominance of spin-wave-like excitations, as assumed in constructing the effective $H_{\mathrm{Heis}}(U)$. For given U/t, $\Omega(\omega)$ is a minimum for the highest of the first N RPA excitations, since the upper band edge therein is most influenced by the encroaching Stoner-like band. Specifically, we find $\Omega(\omega_{\mathrm{max}})=1.00$ down to $U/t\simeq 5$, decreasing to 0.71 for $U/t=3$ and 0.39 for $U/t=2$, although even here the majority of low-ω excitations have $\Omega(\omega)\simeq 1$. Below this, however, $\Omega(\omega_{\mathrm{max}})$ decreases rapidly: Its value is 0.02 for $U/t=1$. The low-ω RPA transverse excitations of the finite-U/t Hubbard model are thus indeed dominated by spin-wave-like excitations for all but the lowest U/t.

The assumptions underlying the approximate mapping of Sec. II are thus supported, yielding quantitatively accurate results over a very wide U/t range encompassing strong-, intermediate-, and weak-coupling strengths, down to U/t of around 2–3. This is in contrast to recent attempts to generalize linear spin wave theory to the Hubbard model. Perturbative methods[26,27] are correct only as $U/t\rightarrow\infty$, i.e., as $J\rightarrow 0$. For large coupling, only the low-ω portion of the spin wave spectrum is given correctly, so that while quantities such as the spin wave velocity (and sublattice magnetization in $d=2$), which are governed by the low-ω portion of the spectrum, are given correctly for large U/t, the full spectrum is not properly obtained, as reflected in, e.g., bulk susceptibilities. A more successful approach[28] considers the poles of $\boldsymbol{\chi}(\omega)$, Eq. (2.26), given by expanding the UHF susceptibility ${}^0\boldsymbol{\chi}$ in powers of t^2/U^2 about the $U\rightarrow\infty$ limit. However, as commented in Ref. 28, convergence of this expansion is slow, such that the approximation in practice remains limited to a large coupling regime.

IV. EFFECTIVE EXCHANGE COUPLINGS

The resultant NN, 2NN, and 3NN exchange couplings obtained from Eq. (2.25) have been shown as a function of U/t for $d=3$ in Fig. 1 of Ref. 21, to which the reader is referred. Decomposing the bipartite simple cubic lattice into two interpenetrating sublattices, the resultant $J_{ij}(U)$'s are found to be positive between i and j on different sublattices, negative between sites on the same sublattice. Thus, AF order is always reinforced, leading to the expectation (examined in Sec. V C) that the resultant Néel temperature will be enhanced over that resulting solely from consideration of nearest-neighbor J_{ij}'s. J_{NN} itself is found to be[21] a maximum for $U/t\simeq 9$, after which it steadily approaches from below the exact strong-coupling asymptote for the Hubbard model, $J_\infty=4t^2/U$. $|J_{2\mathrm{NN}}|$ and $J_{3\mathrm{NN}}$ are always an order of magnitude less than J_{NN} but play a significant role for $U/t\lesssim 15$. One example of this is shown by the upper band edge ω_{max} of N_T^{LSW} (Fig. 2) which, if NN couplings alone were sufficient, would be given by dJ_{NN}. ω_{max} is in fact found to lie somewhat in excess of $3J_{\mathrm{NN}}$, reflecting the role of 2NN and 3NN couplings. The effect is appreciable even for $U/t=12$ and does not become insignificant until $U/t=20$ where (see Fig. 1 of Ref. 21) J_{NN} is close to the strong-coupling asymptote J_∞. Couplings beyond 3NN do of course occur but are found to play only a minor role in practice.

A further illustration of the roles of the various spin couplings at finite U/t is given by considering the effect of zero-point transverse spin fluctuations on the ground state of the effective Heisenberg model. For example, the sublattice magnetization m is obtained readily at a one-loop level (see, e.g., Ref. 14). The known strong-coupling LSW results discussed in Sec. I are correctly recovered, but the present approach permits a study of the effects of low-lying spin waves in reducing m from its mean-field value $m_{\mathrm{HF}}=|\mu|$ [Eq. (3.4)] as a function of interaction strength. Figure 3 thus compares

m to its HF value m_{HF} for the $d=3$ simple cubic lattice. In strong-coupling, $m/m_{\mathrm{HF}}=0.844$, and quantum fluctuations remain fairly significant for interaction strengths down to $\sim U/t=6$, where $m/m_{\mathrm{HF}}\simeq 0.91$. Note, however, that with NN couplings only, the fractional reduction in m depends only on the lattice topology and is independent of the magnitude of J_{NN}, whence m/m_{HF} would retain its strong-coupling value if solely NN interactions were considered. The decrease in the zero-point sublattice magnetization reduction as U/t is lowered thus reflects in part the expected importance of effective exchange couplings beyond purely NN interactions.

V. FINITE-TEMPERATURE MAGNETISM

We turn now to finite-temperature properties of the half-filled Hubbard model, in particular the $(U/t, T/t)$ phase diagram, i.e., the Néel temperature $T_N(U)$ for loss of antiferromagnetic long-ranged order (AFLRO). Granted the mapping on to an effective Heisenberg model, two potential options arise. First, to study finite-T properties via thermal excitation of the low-lying bosonic transverse spin excitations coming from an ordered low-T phase, using familiar linear spin wave theory. This is viable for $d=3$ at temperatures sufficiently deep in the ordered phase, but breaks down progressively with increasing T and yields a poor estimate of T_N. And for $d=2$, the logarithmic divergence of the spin wave amplitude leads at any nonzero T to a divergent magnetization reduction, and hence solely a paramagnetic phase for $T>0$, consistent with the Mermin-Wagner theorem.[11]

An alternative is to approach a possible low-T ordered phase from the "high-T" paramagnet, using the effective $H_{\mathrm{Heis}}(U)$ (whose exchange couplings are not expected to be sensitive to their extraction by comparison of linearized theories, RPA and LSW). It is this route we take, although something more than a molecular-field-type theory for $H_{\mathrm{Heis}}(U)$ is clearly required if justice is to be done to paramagnetic spin correlations and the dictates of the Mermin-Wagner theorem satisfied: This is provided by the Onsager reaction field[17] (ORF) approach outlined in Sec. V B. First, however, we comment briefly on the finite-T UHF mean-field state, and anticipate thermal implications of the separation of energy scales for spin-wave-like and Stoner-like excitations, as found in Sec. III.

A. UHF for $T>0$

Extension of UHF to finite T is straightforward, consisting simply of a variational minimization of the UHF free energy functional.[29,30] Our first point concerns the particle-hole stability of the resultant self-consistent solutions which is necessary in order that collective excitations about the mean-field state be bounded.[31] This is important, for it has been argued (see, e.g., Ref. 30) that for finite T there will exist 2^N possible stable UHF states, each Ising-like and constructed essentially from the pure Néel state by flipping any number of the mean-field local moments. However, from extensive numerical work on large finite-size systems, we have found this not to be the case. That is, while many Ising-like self-consistent solutions to the UHF equations may exist at a given temperature, only the pure two-sublattice Néel state (and its spin-flipped image) is properly stable against particle-hole excitations —i.e., is a true minimum of the UHF free energy surface. The temperature-dependent local moment magnitude corresponding to this solution is given by the finite-T analog of Eq. (3.4), i.e.,

$$1=\frac{U}{N}\sum_{\mathbf{q}\in \mathrm{MBZ}}\frac{\tanh[E_{\mathbf{q}}(\Delta)/2kT]}{E_{\mathbf{q}}(\Delta)}\,, \tag{5.1}$$

where $E_{\mathbf{q}}(\Delta)=[\frac{1}{4}\Delta^2+\epsilon_{\mathbf{q}}^2]^{1/2}$ and $\Delta(T)=U|\mu(T)|$. Equation (5.1) has a nonzero solution for $|\mu(T)|$ below a critical temperature $T_{\mathrm{HF}}(U)$, at which Stoner-like thermal excitations across the single-particle gap destroy the UHF local moments. [Above $T_{\mathrm{HF}}(U)$, the sole solution to the UHF equations is the paramagnetic or restricted HF solution.] This clearly occurs at a temperature scale on the order of the single-particle gap $\Delta(0)=U|\mu(0)|$; in fact, $T_{\mathrm{HF}}(U)$ from Eq. (5.1) goes asymptotically as $\frac{1}{4}U$, an asymptote closely approached in practice for $U/t\gtrsim 4$ or so.

It is of course clear that $T_{\mathrm{HF}}(U)$ tells us essentially nothing about the true Néel temperature $T_N(U)$ for destruction of AFLRO in $d=3$, save for the weakest interaction strengths. The energy scale for disordering of the *orientations* of local moments is set by the effective coupling constants $J_{ij}(U)$ and not the single-particle band gap $\Delta(0)$ of order U. However, we can simply but readily include the first effects of thermal excitations across the gap on the local moment *magnitudes* by replacing the zero-temperature $|\mu_i|$'s entering Eq. (2.25b) for the effective coupling constants by their self-consistent, finite-T values given by Eq. (5.1). This has a non-negligible effect on $T_N(U)$ only for interaction strengths $U/t\lesssim 4$, but ensures a sensible interpolation between weak and strong interaction limits.

$T_{\mathrm{HF}}(U)$ sets a natural upper T limit for the theory we develop. However, save for the lowest U/t, T_{HF} is sufficiently in excess of $T_N(U)$ that there exists a wide T interval —extending at least to several times T_N itself— over which thermodynamic properties are dominated by the low-energy spin scale captured in the effective $H_{\mathrm{Heis}}(U)$, and are barely affected by the high-energy Stoner-like processes. This will be shown explicitly in Sec. V D.

B. Onsager reaction field theory

We now sketch an Onsager reaction field (ORF) treatment of the effective Heisenberg model, Eq. (2.25), with U-dependent exchange couplings $\{J_{ij}(U)\}$. Full details are given in a recent paper,[40] to which the reader is referred. ORF provides an essential modification of molecular field (MF) theory by incorporating self-consistently the vital effects of short-ranged magnetic ordering in the paramagnetic phase. Originally devised in the context of dielectric theory by Onsager,[17] it was first extended to magnetism by Brout and Thomas[32] and has since been applied successfully to eg spin glasses[33,34] and itinerant electron systems.[35–38]

Approaching $T_N(U)$ from the paramagnetic phase, the required modification of MF theory stems from a recognition[17] that the MF acting on a given spin, $\mathbf{h}_i^{\mathrm{MF}}=\Sigma_j J_{ij}\langle \mathbf{S}_j\rangle$ (where $\langle\cdots\rangle$ now denotes a thermal average), is itself a sum of two fields: the cavity field $\mathbf{h}_i^{\mathrm{CF}}$, which is the field in the absence of the given spin, and the reaction field $\mathbf{h}_i^{\mathrm{RF}}$, arising due to

polarization of its neighbors by the spin itself. $\mathbf{h}_i^{\mathrm{RF}}$ is given by $\mathbf{h}_i^{\mathrm{RF}}=\lambda\langle\mathbf{S}_i\rangle$ with $\lambda(T)=\Sigma_j J_{ij}\langle\mathbf{S}_i\cdot\mathbf{S}_j\rangle/S(S+1)$ ($S=\frac{1}{2}$ here). But since the reaction field is parallel to the spin, it cannot contribute to its own alignment. It must therefore be removed from the MF, whence the cavity field $\mathbf{h}_i^{\mathrm{CF}}=\mathbf{h}_i^{\mathrm{MF}}-\mathbf{h}_i^{\mathrm{RF}}$ —and not the MF— is the correct local field to which the spin responds, and this must of necessity be implemented self-consistently, since the ORF depends on the local spin correlations, embodied in $\lambda(T)$.

The static susceptibility $\chi(\mathbf{q})$ is then obtained in direct analogy to standard MF theory, and by imposing self-consistently the fluctuation-dissipation theorem $\langle\mathbf{S}_i\cdot\mathbf{S}_j\rangle=3T\chi_{ij}$ one obtains[40]

$$\frac{T_N^{\mathrm{MF}}(U)}{T}=N^{-1}\sum_{\mathbf{q}}\,[z-J(\mathbf{q})/J(\boldsymbol{\pi})]^{-1}\equiv G(z). \quad (5.2)$$

Here, $T_N^{\mathrm{MF}}(U)=1/4|J(\boldsymbol{\pi})|$ is the molecular field ($\lambda=0$) Néel temperature, with $J(\mathbf{q})$ the Fourier transform of $\{J_{ij}(U)\}$ and $z=(T/T_N^{\mathrm{MF}})+[\lambda/J(\boldsymbol{\pi})]$. Equation (5.2) determines $z(T)$ [or equivalently $\lambda(T)$] self-consistently, the temperature scale being set by $T_N^{\mathrm{MF}}(U)$. The $\chi(\mathbf{q})$ then follow directly from[40] $|J(\boldsymbol{\pi})|\chi(\mathbf{q})=[z(T)-J(\mathbf{q})/J(\boldsymbol{\pi})]^{-1}$, and since $\chi(\mathbf{q})$ first diverges for $\mathbf{q}=\boldsymbol{\pi}$ at $z(T)=1$, the ORF Néel temperature is given by

$$T_N(U)=T_N^{\mathrm{MF}}(U)/G(z=1+). \quad (5.3)$$

Spin correlation functions in the paramagnetic phase likewise follow from $\langle\mathbf{S}_i\cdot\mathbf{S}_j\rangle/3T=G_{ij}(z)/|J(\boldsymbol{\pi})|$ where

$$G_{ij}(z)=N^{-1}\sum_{\mathbf{q}}\,e^{i\mathbf{q}\cdot\mathbf{R}_{ij}}[z-J(\mathbf{q})/J(\boldsymbol{\pi})]^{-1}. \quad (5.4)$$

Mathematically, the $G_{ij}(z)$'s are formally equivalent to the site Green functions for an arbitrary one-band tight-binding Hamiltonian in d dimensions, with $G(z)\equiv G_{ii}(z)$. Therefore, $G(z\to1+)$ diverges algebraically in $d=1$ and logarithmically in $d=2$.[39] This result is not confined solely to NN coupling constants (and thus the strong-coupling limit), and implies the absence of AFLRO in $d\leqslant2$ for $T>0$, consistent with the Mermin-Wagner theorem.[11] Although our main focus here is a determination of $T_N(U)$ for the Hubbard model in $d=3$, note that the logarithmic divergence of $G(z\to1+)$ for $d=2$ leads directly as $T\to0$ to an exponentially divergent spin correlation length $\xi(T)$, indicative of the AFLRO characteristic of the $T=0$ ground state. In the strong-coupling limit $U/t\to\infty$, this reduces asymptotically for $T\to0$ to

$$\xi(T)=C\exp(\pi T_N^{\mathrm{MF}}/2T)\equiv C\exp(2\pi\rho_s/T), \quad (5.5)$$

where C is a T-independent constant, and $\rho_s=\frac{1}{4}T_N^{\mathrm{MF}}=\frac{1}{4}J_\infty$ ($J_\infty=4t^2/U$) is also the $T=0$ spin-stiffness constant obtained from LSW about the AF-ordered Néel state of the $d=2$ pure nearest-neighbor Heisenberg model. The asymptotic form of Eq. (5.5) agrees with the two-loop order calculation by Chakravarty, Halperin, and Nelson[41] on the quantum nonlinear σ model in $2+1$ dimensions, and the success of an ORF approach in $d=2$, compared to quantum Monte Carlo and other analytical approaches, is detailed in Ref. 40.

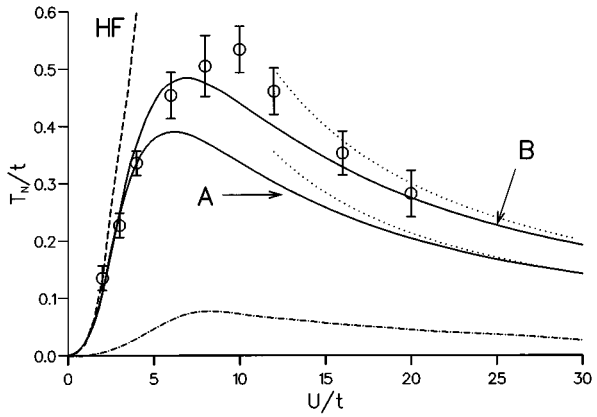

FIG. 4. Néel temperature vs U/t. (A) Onsager reaction field T_N, (B) molecular field T_N^{MF}. Also shown are QMC results (Ref. 18) (circles), the strong-coupling asymptotes $T_N^{\mathrm{MF}}\to6t^2/U$ and $T_N\to3.96t^2/U$ from ORF theory, T_{HF} (dashed line), and the VF (Refs. 42,43) result (dot-dashed line).

C. Phase diagram of $d=3$ Hubbard model

For $d=3$, numerical evaluation of $G(1)$ using the U/t-dependent exchange couplings yields directly $T_N(U)$ via Eq. (5.3). In Fig. 4 we show the $(U/t,T/t)$ phase diagram obtained from both MF and ORF methods. Clearly, the effects of short-ranged spin correlations, self-consistently included in the ORF treatment, are crucial in reducing $T_N(U)$ from its MF value for all but the weakest interaction strengths U/t. In strong coupling $U/t\to\infty$, MF theory yields the expected $T_N^{\mathrm{MF}}\to6t^2/U$, while the ORF $T_N\to3.96t^2/U$, which is within 3% of the accepted value of $3.83t^2/U$ obtained from high-temperature series expansions (HTSE's),[10] and in the weak-coupling limit T_N approaches the expected [3–9,18] $T_{\mathrm{HF}}(U)$, so that the treatment interpolates sensibly between weak- and strong-coupling regimes.

Figure 4 compares our results for T_N with the Néel temperature of the $d=3$ Hubbard model inferred from QMC calculations by Scalettar *et al.*;[18] for $U/t\gtrsim6-8$, these results are significantly reduced from earlier QMC work by Hirsch[19] on smaller lattices. Clearly, the QMC points are well reproduced by the *molecular field* $T_N^{\mathrm{MF}}(U)$ over the entire U/t range, our estimate being within the MC error bars for all but two points ($U/t=10,12$ although even here it is close). Further, by $U/t=20$, the QMC results appear to be approaching the MF asymptote and remain well above the HTSE limit. These observations lend weight to Hasegawa's argument[7] that the extrapolation used to extract T_N from the QMC data yields a Weiss temperature (rather than the true T_N) —which is precisely the quantity obtained by MF theory— and therefore overestimates T_N. In Fig. 4 therefore, we believe that T_N^{MC} should be compared with T_N^{MF} rather than the ORF Néel temperature. This does not, however, presage poor agreement between QMC and the ORF approach, for a reliable determination of the Néel temperature from QMC calculations on relatively small systems is clearly difficult; a more revealing comparison is provided by the T dependence of, e.g., the spin correlation functions, considered in the following section.

Previous functional integral approaches mentioned in Sec. I include the single-site spin fluctuation theory of Hubbard[3]

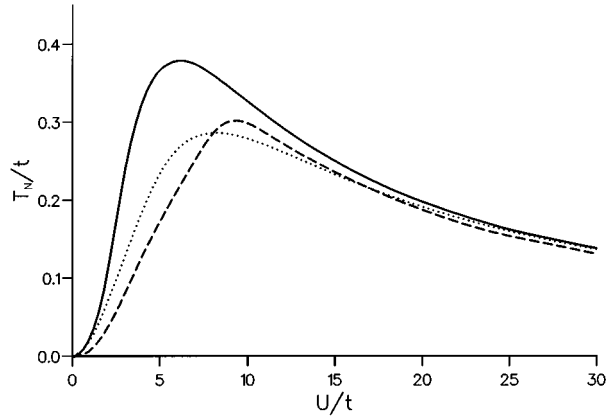

FIG. 5. ORF T_N (solid line), T_N for solely NN J_{ij}'s (dotted line) and the postulated form for the true T_N from Ref. 6 (dashed line).

and Hasegawa,[4] the Gutzwiller-type variational approach of Kakehashi, Fulde, and Samson,[5] and a more recent treatment by Hasegawa.[7] Comparison of these with the present theory has been given in a previous paper[21] (Fig. 3); none reproduces the QMC results nearly as well as the simple $T_N^{\mathrm{MF}}(U)$ above. More significantly, however, these approaches share the common deficiency that all yield the molecular field asymptote $T_N^{\mathrm{MF}}(U)$ in strong coupling. We believe this to be a serious limitation even down to relatively low U/t since, as shown by Fig. 4, the effects of spin correlations included in the ORF treatment reduce significantly $T_N(U)$ below its MF value over a wide U/t range.

A previous attempt to include such effects has been made by Moriya and co-workers;[42,43] their "vector field" (VF) method aims to include the dominant effects of short-ranged magnetic order omitted by the above approaches. Unfortunately, as shown by Fig. 4, the estimated $T_N(U)$ appears seriously awry over the entire U/t range, and the model contains several unphysical properties.[6] But we believe the present results do support the necessity of including spin correlations, and provide possibly the simplest, qualitatively correct means of so doing.

Finally, it is interesting to note that our ORF results agree rather well with Kakehasi and Hasegawa's[6] conjectured form for the true $T_N(U)$. Figure 5 shows the ORF $T_N(U)$, together with the analogous result obtained by constraining the effective exchange couplings to be purely NN, and the pos-

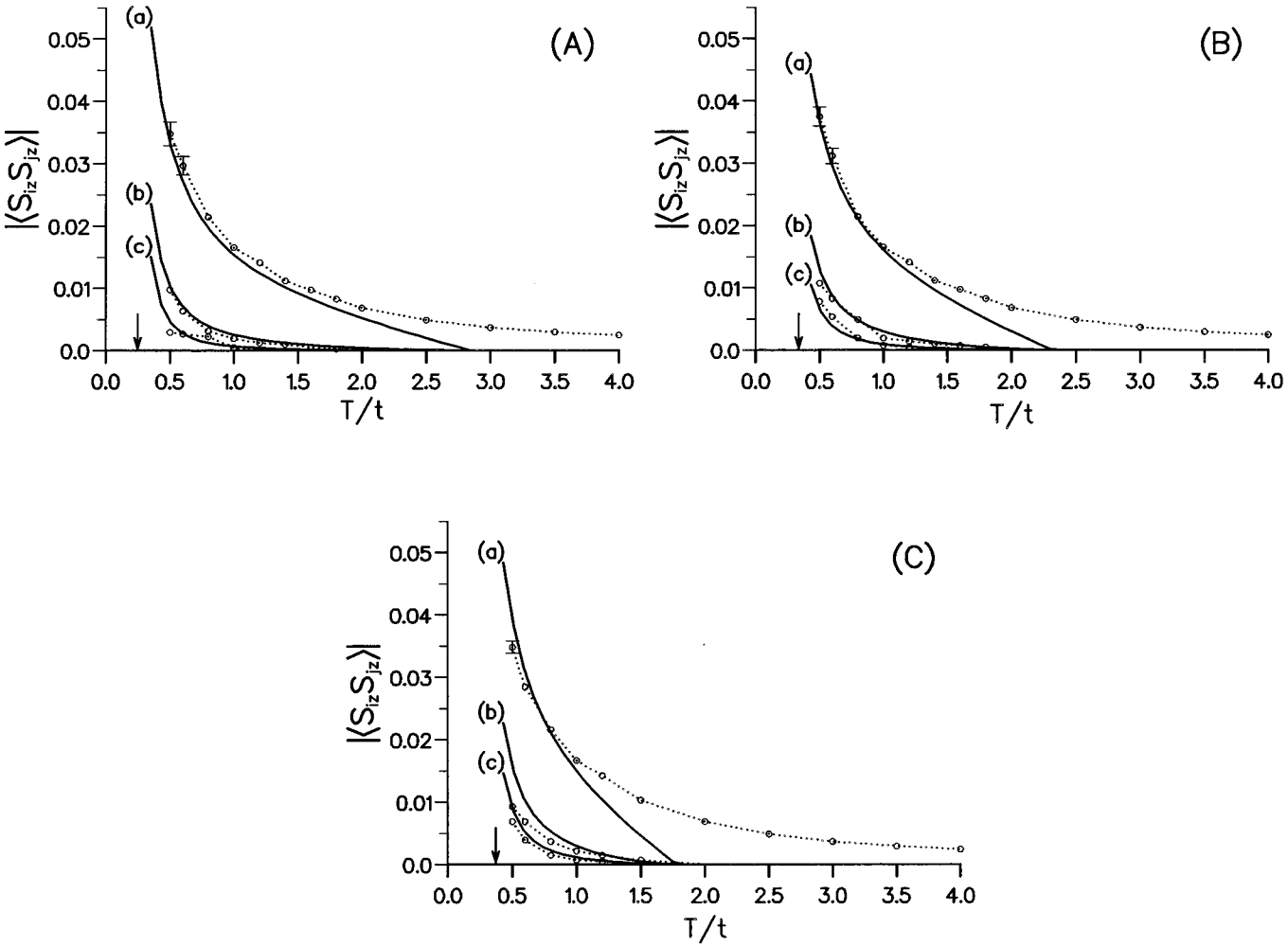

FIG. 6. Spin correlation functions $|\langle S_{iz}S_{jz}\rangle|$ vs T/t in the paramagnet for $U/t=12$ (A), 10 (B), and 8 (C). The ORF Néel temperature T_N is indicated by an arrow. (a) Nearest neighbor, (b) 2NN, (c) 3NN. Circles show QMC results (Ref. 19).

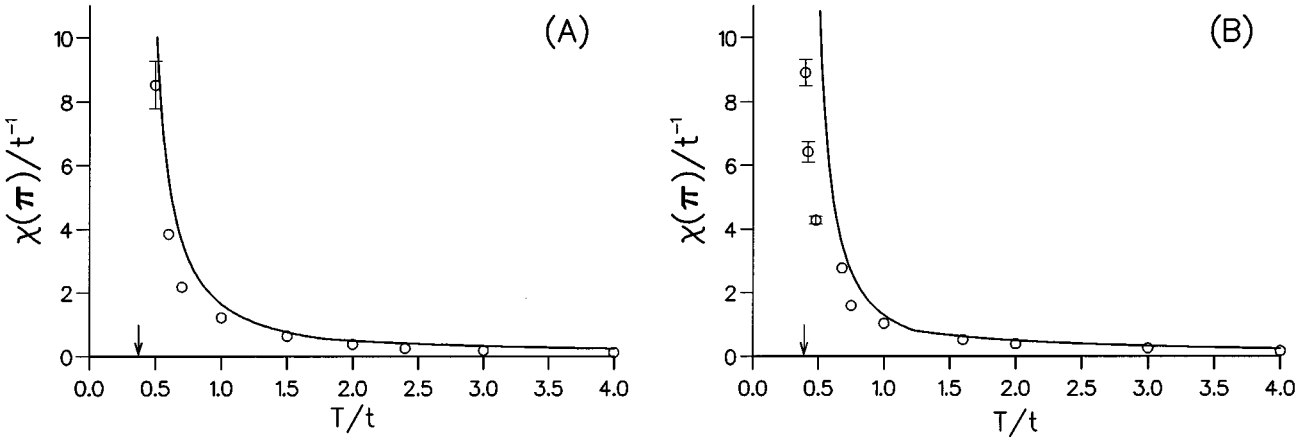

FIG. 7. Staggered susceptibility $\chi(\boldsymbol{\pi})$ vs T/t for $U/t=8$ (a) and 6 (b). The ORF Néel temperature T_N is indicated by an arrow. Also shown are QMC results (circles) from Ref. 19 (a) and Ref. 18 (b).

tulated form from Ref. 6. The agreement between the latter and the NN curve is remarkably good. In addition, the effects of couplings beyond NN in stabilizing the AF phase are particularly clear here, the full ORF $T_N(U)$ being significantly enhanced over its pure NN counterpart, and giving much better agreement with QMC results in the weak-coupling regime.

D. Paramagnetic phase

Given the importance of a good description of short-ranged order as stressed above, it is important to examine whether the present theory describes well the temperature dependence of intersite spin correlation functions (SCF's) in the paramagnetic phase. Within a molecular field approximation these vanish by definition in the paramagnet, and so all correlation stems from the nontrivial effects of the reaction field. Figure 6 shows the T dependence of $\langle S_{iz}S_{jz}\rangle$ $(=\frac{1}{3}\langle \mathbf{S}_i\cdot\mathbf{S}_j\rangle)$ for $T\geqslant T_N(U)$, for three values of the interaction strength $U/t=12$, 10, and 8. NN and 3NN spin correlations are always negative and the 2NN SCF always positive, as expected, and so $|\langle S_{iz}S_{jz}\rangle|$ is shown; these are compared to Hirsch's[19] QMC results for the half-filled Hubbard model on a 4^3 lattice. It is clear in each case that appreciable spin correlations beyond NN build up only for temperatures $T/t\lesssim 1$, and agreement with QMC is noticeably poorer if the effective exchange couplings $\{J_{ij}(U)\}$ are constrained solely to nearest-neighbors. For $U/t=12$, the ORF results of Fig. 6(a) agree well with QMC over a very wide T range above the ORF $T_N(U)\simeq 0.29t$ (despite the aforementioned disparity between the two estimates of T_N). For the NN $\langle S_{iz}S_{jz}\rangle$, the agreement becomes poorer only for temperatures approaching $T_{HF}(U)\simeq 3t$ at which the UHF local moments are thermally destroyed. This is precisely as expected for, as discussed above, $T_{\rm HF}(U)$ represents a definite upper limit for the theory, setting a thermal scale for the Stoner-like excitations neglected in the effective $H_{\rm Heis}(U)$. For $U/t=12$, $T_{\rm HF}$ is an order of magnitude greater than the Néel temperature. It diminishes with decreasing U/t (see Fig. 4), whence the T interval over which good agreement with QMC is obtained naturally becomes narrower [Figs. 6(b), 6(c)]. However, as seen from Fig. 6 —on which the ORF $T_N(U)$ is also marked— the temperature interval over which the QMC spin correlations seem well captured extends up to $\sim$3–4 times T_N itself and thus, while narrower on the hopping scale t (as used in the figure), remains appreciable in real terms. (One should also bear in mind that with decreasing U/t, system-size effects in QMC are likely to become more significant.)

To illustrate the resultant static susceptibilities, Fig. 7 shows the ORF staggered $\chi(\boldsymbol{\pi})$ vs T/t for (a) $U/t=8$ and (b) $U/t=6$. The former is compared to Hirsch's QMC results[19] for the half-filled Hubbard model on a 6^3 lattice, the latter to Scalettar *et al.*[18] on a 8^3 lattice. The agreement is rather good, even for the lower temperatures where system-size effects in QMC have a not insignificant effect [see Fig. 10(b) of Ref. 19]; although the ultimate high-T asymptote of the QMC susceptibilities must correctly be one-half the free-spin Curie law (as for the noninteracting limit), whereas a pure Curie law naturally results for the effective $H_{\rm Heis}(U)$. A similar quality of comparison results for the uniform $\chi(\mathbf{0})$. We also expect the agreement to improve with increasing U/t, but unfortunately QMC results for $U/t>8$ do not appear to have been reported.

Finally, to illustrate the effect on thermodynamic properties of the scale separation between low-energy spin excitations embodied in the effective $H_{\rm Heis}(U)$ and the omitted higher-energy Stoner-like excitations, Fig. 8 shows the ORF entropy $S(T)$ vs $T/T_N(U)$ for $U/t=10$, as obtained from the integrated specific heat. This is readily shown to be given by

$$S(T)=S(T_N)-\frac{3}{2}\left[1-\frac{T_N^{\rm MF}(U)}{T_N(U)}+\frac{\lambda(T)}{4T}\right]-\frac{3}{8}\int_{T_N(U)}^{T}\frac{\lambda(T)}{T^2}dT, \tag{5.6}$$

with the ORF $\lambda(T)$ determined self-consistently for the chosen U/t as outlined in Sec. V B. The molecular field limit of Eq. (5.6) is, trivially, $\lambda(T)=0$ and $T_N\equiv T_N^{\rm MF}$, whence $S(T)\equiv S(T_N^{\rm MF})=R\ln 2$ throughout the paramagnetic phase. To estimate $S(T_N)$ at the ORF level, we impose the constraint $S(T_{\rm HF})=R\ln 2$ with the T dependence of $|\mu(T)|$ included in the effective exchange couplings [since from Eq. (2.25b) the $\{J_{ij}\}$ are effectively "switched off" when the local moments vanish as $T\rightarrow T_{\rm HF}(U)-$]. Alternatively, if the

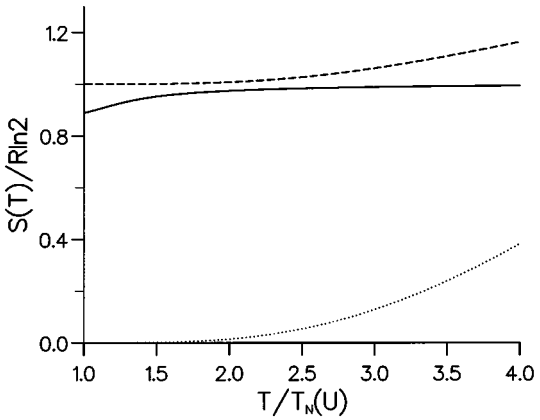

FIG. 8. ORF entropy vs $T/T_N(U)$ for $U/t=10$ in the paramagnetic phase (solid line), compared to the mean-field entropy $S_0(T)$ [Eq. (5.10), dotted line], and the atomic limit entropy $S_{\mathrm{AL}}(T)$ (dashed line).

$T=0$ $|\mu(0)|$ is used, one demands that $S(T)\rightarrow R\ln 2$ as $T\rightarrow\infty$. The two estimates of $S(T_N)$ differ negligibly for $U/t=10$ (as also for $U/t=8,6$), as expected from the discussion of Sec. V A. The resultant $S(T)$ saturates in practical terms to $R\ln 2$ on a T scale of ~ 2–3 times $T_N(U)$, commensurate with the behavior of the corresponding spin correlations, Fig. 6(b).

For comparison, Fig. 8 shows the pure mean-field reference entropy $S_0(T)$ given by

$$S_0(T)=-R\int_{-\infty}^{\infty} dED(E)\{f(E)\ln f(E) + [1-f(E)]\ln[1-f(E)]\}, \tag{5.7}$$

where $D(E)$ is the UHF single-particle spectrum. $S_0(T)$ includes only excitations across the single-particle band gap in $D(E)$, and naturally fails to describe the low-energy transverse spin excitations, but its value gives an (over)estimate of the residual contribution to $S(T)$ arising from the Stoner-like excitations neglected in the effective $H_{\mathrm{Heis}}(U)$. As seen from the figure, these begin to become appreciable only on a T scale exceeding that at which the ORF $S(T)$ effectively reaches its free-spin value. It is also instructive to compare $S(T)$ to the exact atomic limit ($t=0$) entropy, $S_{\mathrm{AL}}(T)$ (Fig. 8), which starts from a value of $R\ln 2$ at $T=0+$ and, like $S_0(T)$, eventually reaches $R\ln 4$ at a temperature of order U where excitations across the single-particle gap U begin to saturate. As seen from Fig. 8, however, the latter effect is again not significant over the temperature regime on which we have focused.

VI. CONCLUSION

The present work provides a physically transparent and seemingly successful approach to low-energy spin excitations in the half-filled Hubbard model and their thermodynamic consequences.

A mapping of the low-energy transverse spin excitations of the model onto those of an effective underlying Heisenberg model, which is of course exact in strong-coupling, is found to be quantitatively accurate over a very wide range of interaction strengths down to weak coupling U/t of around 2–3, as judged by comparison with the full RPA transverse spin spectrum for the antiferromagnetic broken symmetry state.

Physical properties of the system in the thermal paramagnetic phase have been described via a simple Onsager reaction field approach, which demonstrates clearly the importance of describing self-consistently spin correlations in the paramagnet. This is central, in recovering, for example, the dictates of the Mermin-Wagner theorem for $d\leqslant 2$ and for $d=3$ (where resultant ORF exponents are spherical[40]) in describing, for example, the phase boundary to AFLRO where, for strong coupling in particular, excellent agreement with known high-temperature series expansion results is obtained. Further, the separation of energy scales between low-energy spin-wave-like excitations and higher-energy Stoner-like processes, which is found to persist over a very wide range of interaction strengths down to weak coupling U/t, is manifest thermally in an appreciable temperature range above $T_N(U)$ over which physical properties appear dominated by the low-lying transverse spin excitations. As judged in particular by comparison with a range of quantum Monte Carlo results for the Hubbard model these are rather well described by the present work, which appears to represent a significant improvement over previous approaches.

Finally, we note that neither the mapping on to an effective underlying Heisenberg model nor the subsequent ORF approach is confined to the pure Hubbard model on which we have concentrated here, but can be adapted readily to magnetically ordered phases of disordered Hubbard models, as will be discussed in a later publication.[20]

ACKNOWLEDGMENTS

Y.H.S. would like to thank Dr. M. J. Attenborough for helpful discussions. We thank the SERC, EPSRC (Condensed Matter Physics), and the Royal Commission for the Exhibition of 1851 for financial support.

[1] P. W. Anderson, *Concepts in Solids* (Benjamin, Reading, MA, 1963).

[2] E. Manousakis, Rev. Mod. Phys. **63**, 1 (1991).

[3] J. Hubbard, Phys. Rev. B **19**, 2626 (1979); **20**, 4584 (1979); **23**, 5970 (1981).

[4] H. Hasegawa, J. Phys. Soc. Jpn. **46**, 1504 (1979); **49**, 178 (1980).

[5] Y. Kakehashi and P. Fulde, Phys. Rev. B **32**, 1595 (1985); Y. Kakehashi and J. H. Samson *ibid.* **33**, 298 (1986).

[6] Y. Kakehashi and H. Hasegawa, Phys. Rev. B **36**, 4066 (1987); **37**, 7777 (1988).

[7] H. Hasegawa, J. Phys. Condens. Matter **1**, 9325 (1989).

[8] *Electron Correlations and Magnetism in Narrow Band Systems*,

edited by T. Moriya (Springer, Berlin, 1981).
[9] T. Moriya, *Spin Fluctuations in Itinerant Electron Magnetism* (Springer, Berlin, 1985).
[10] G. S. Rushbrooke, G. A. Baker, and P. J. Wood, in *Phase Transitions and Critical Phenomena*, edited by C. Domb and M. S. Green (Academic, New York, 1974), Vol. 3, Chap. 5.
[11] N. D. Mermin and H. Wagner, Phys. Rev. Lett. **22**, 1133 (1966); P. C. Hohenberg, Phys. Rev. **158**, 383 (1967).
[12] A. Singh and Z. Tesanović, Phys. Rev. B **41**, 614 (1990); **41**, 11457 (1990).
[13] J. R. Schrieffer, Z.-G. Wen, and S.-C. Zhang, Phys. Rev. B **39**, 11663 (1989).
[14] D. C. Mattis, *The Theory of Magnetism* (Springer, Berlin, 1988).
[15] Y. H. Szczech, M. A. Tusch, and D. E. Logan (unpublished).
[16] D. R. Penn, Phys. Rev. **142**, 350 (1966).
[17] L. Onsager, J. Am. Chem. Soc. **58**, 1486 (1936).
[18] R. T. Scalettar, D. J. Scalapino, R. L. Sugar, and D. Toussaint, Phys. Rev. B **39**, 4711 (1989).
[19] J. E. Hirsch, Phys. Rev. B **35**, 1851 (1987).
[20] Y. H. Szczech, M. A. Tusch, and D. E. Logan (unpublished).
[21] Y. H. Szczech, M. A. Tusch, and D. E. Logan, Phys. Rev. Lett. **74**, 2804 (1995).
[22] M. A. Tusch and D. E. Logan, Phys. Rev. B **48**, 14843 (1993).
[23] A. L. Fetter and J. D. Walecka, *Quantum Theory of Many-Particle Systems* (McGraw-Hill, New York, 1971).
[24] K. Yonemitsu, I. Batistić, and A. R. Bishop, Phys. Rev. B **44**, 2652 (1991).
[25] D. G. Rowan, Y. H. Szczech, M. A. Tusch, and D. E. Logan, J. Phys. Condens. Matter **7**, 6853 (1995).
[26] X.-Z. Yan, Phys. Rev. B **46**, 9231 (1992); **45**, 4741 (1992).
[27] H.-Y. Choi, Phys. Rev. B **44**, 2609 (1991).
[28] A. Singh, Phys. Rev. B **48**, 6668 (1993).
[29] See, e.g., P. G. de Gennes, *Superconductivity of Metals and Alloys* (Benjamin, New York, 1966); M. Brack and P. Quentin, Phys. Lett. **52B**, 159 (1974).
[30] B. H. Brandow, Adv. Phys. **26**, 651 (1977).
[31] D. J. Thouless, *The Quantum Mechanics of Many-Body Systems* (Academic, New York, 1972).
[32] R. Brout and H. Thomas, Physics (Long Island City, N.Y.) **3**, 317 (1967).
[33] M. Cyrot, Phys. Rev. Lett. **43**, 173 (1979).
[34] P. Nozières, J. Phys. (Paris) **43**, L543 (1982).
[35] M. Cyrot, in Ref. 8, p. 51.
[36] J. B. Staunton and B. L. Gyorffy, Phys. Rev. Lett. **69**, 371 (1992).
[37] A. Georges and J. S. Yedidia, Phys. Rev. B **43**, 3475 (1991).
[38] P. Kopietz, Phys. Rev. B **48**, 13789 (1993).
[39] E. N. Economou, *Green's Functions in Quantum Physics* (Springer, Berlin, 1983).
[40] D. E. Logan, Y. H. Szczech, and M. A. Tusch, Europhys. Lett. **30**, 307 (1995).
[41] S. Chakravarty, B. I. Halperin, and D. R. Nelson, Phys. Rev. B **39**, 2344 (1989).
[42] T. Moriya and Y. Takahashi, J. Phys. Soc. Jpn. **45**, 397 (1978).
[43] T. Moriya and H. Hasegawa, Phys. Soc. Jpn. **48**, 1490 (1980).